CrossMark

Preparation and thermal cycling of expanded graphite/adipic acid composite phase change materials

Weibing Zhou[1,2] · Kang Li[1] · Jiaoqun Zhu[1] · Ruguang Li[1] · Xiaomin Cheng[2] ·
Fengli Liu[2]

Abstract Expanded graphite (EG)/adipic acid (AA) composite phase change materials were prepared in the paper. The structure and properties of composite were investigated by FTIR, DSC and FE-SEM. The results showed AA can be adsorbed into the structure of the expanded graphite. Meanwhile, they exhibited good compatibility. With the content of EG increased, the latent heat and thermal conductivity of the composites were decreased. When the content of EG is 10 mass%, the thermal conductivity of composites was 4.35 W m^{-1} K^{-1}, which was obviously higher than pure adipic acid. The melting and freezing latent heats of AA were 220.2 and 220.5 J g^{-1}, decreasing 16.1 and 13.7% after 1000 times thermal cycling. The results showed the composites had good thermal stability.

Keywords Adipic acid · Expanded graphite · Latent heat · Thermal conductivity · Thermal cycling

Introduction

Phase change materials (PCMs) have a high heat of fusion, and phase change process at a constant temperature, which is suitable for storing or releasing large amounts of thermal energy [1–3]. Organic phase change materials are excellent due to the slight supercooling and phase segregation [4–7]. However, the thermal conductivity of most organic PCMs is just about 0.2 W m^{-1} K^{-1}, which limits the application of latent thermal storage technology in practical thermal storage system. A series of modified techniques have been proposed to improve thermal conductivities, such as high thermal conductivity materials be added into the PCMs. The adding materials include copper, aluminum, carbon nanofibers, carbon nanotubes and expanded graphite (EG) [8–14].

EG has some advantages, especially for nanometer in thickness and micrometer in diameter, which could form thermal conducting network in matrix compared with traditional particle fillers. Therefore, EG has been considered as one of the most excellent heat transfer promoters in thermal storage fields [15–19]. Recently, EG has been used as additive to improve the thermal conductivity of composite materials. Sari and Karaipekli [17] have prepared palmitic acid (PA)/expanded graphite (EG) form-stable phase change composite materials. Thermal conductivity of form-stable PA/EG composites is 2.5 times higher than that of pure PA. Thermal cycling test showed that the composite PCMs have good thermal reliability after 3000 times thermal cycling. Ke et al. [18] studied the heat transfer behavior of the paraffin/EG composite materials, and the paraffin was impregnated into the matrix by capillary action. The thermal conductivities of these composites were found as high as 70 W m^{-1} K^{-1}, depending on the graphite density and orientation. Fang et al. [19]

✉ Weibing Zhou
  jsyczwb@whut.edu.cn

✉ Ruguang Li
  liruguang2005@163.com

[1] State Key Laboratory of Silicate Materials for Architectures, Wuhan University of Technology, Wuhan 430070, People's Republic of China

[2] School of Materials Science and Engineering, Wuhan University of Technology, Wuhan 430070, People's Republic of China

reported the synthesis and characteristics of the stearic acid (SA)/expanded graphite (EG) composites as thermal energy storage materials. When the content of EG in the composites is 17 mass%, the thermal conductivity of the composites is 10 times higher than that of pure SA. All the results found that addition of EG could effectively improve the thermal conductivity of organic heat storage materials.

Meanwhile, adipic acid (AA) is the most important commercialized dicarboxylic acid. It has been manufactured worldwide on a large scale, which primary applied in the production of nylon66 polyamide. The other miscellaneous applied fields are adhesives, insecticide, tanning and dying, and textile industries [20]. Actually, AA is the most appropriate candidate as PCM for cheap, widely available, thermally stable, considerable latent heat and not harmful for the nature. Therefore, it has been attracted the wide attraction in thermal storage fields. Zhu et al. [21] prepared the adipic acid–amorphous silica composite phase change thermal energy materials through using a hydrothermal method. Seki et al. [22] prepared the binary mixture of adipic acid (AA) and sebacic acid (SA) by adding the graphite nanoplates (GNP) to decrease the extent of supercooling and improve the thermal conductivity. Liu et al. [23] also investigated the phase transition behavior of adipic acid as a function of silica pore size. In all, there are relatively fewer reports to use adipic acid as heat storage materials. In the present work, adipic acid was used as phase change material and expanded graphite (EG), with its content ranging from 0 to 10 mass%, was taken into adipic acid to improve its thermal conductive material. The effects of EG on the thermo-physical properties of the composite PCMs, such as the thermal conductivity, phase change temperature and latent heat, were investigated. Additionally, thermal cycling stability of EG/AA composite PCMs was also researched in the paper.

Experimental

Materials

Pure adipic acid (AA) was purchased from Alartin Chemical Reagent Co. Ltd. and without further purification. The melting point (T_m) and latent heat enthalpy (ΔH_m) were 151–155 °C and 260 J g^{-1}, respectively. The properties of AA are shown in Table 1.

Preparation

Preparation of EG

The raw expandable graphite (80 mesh, type A895, Qingdao Tianhe Graphite Co. Ltd.) was subjected to heat treatment in

Table 1 Thermo-physical properties of AA

Parameters	Values
Chemical formula	$C_6H_{10}O_4$
Molecular weight	146.14
Melting point/°C	151–155
Specific heat/J g^{-1} K^{-1}	1.55
Heat of fusion/J g^{-1}	260
Density/g cm^{-3}	1.36
Thermal conductivity/W m^{-1} K^{-1}	0.45

muffle furnace at 800 °C for 5 min. Then the product was mixed and immersed in a alcohol solution consisting of alcohol and distilled water, with the volume ratio of 7:3 for 12 h. Further, the mixture was subjected to ultrasonic irradiation with a power of 100 W for 8 h and EG was obtained finally. The magnified image of EG is shown in Fig. 1a, and the volume was obviously bigger than that of its initial.

Preparation of EG/AA composite PCMs

In this study, adipic acid (AA) is chemical grade with the purity of 99.8%. The composite PCMs were fabricated by mechanical mixing and melted adsorption method. Firstly, the composites with different mass fraction of EG were mechanically mixed for 20 min and then placed in drying closet under 160 °C for 6 h. Secondly, the mixtures were smashed to pieces and placed to tube and later they were heated at 180 °C and stirred through a roll mixer for 2 h. Finally, the uniform mixtures were taken out and grinded into powder for experiment test.

Thermal cycling test

Thermal compatibility of EG/AA composite PCMs was investigated by thermal cycling tests. The variations of latent heat and phase change temperatures were determined after thermal cycling. After 100, 300, 600 and 1000 thermal cycles, the chemical and thermal stabilities of EG/AA composite PCMs were investigated by DSC and FTIR analyses. DSC analyses were performed with a heat rate of 5 °C min^{-1} and the temperature in the range from room temperature to 200 °C under a constant stream of nitrogen.

Before the thermal cycling test, pure AA and 8 mass% EG/AA were selected and subjected to thermal cycling in the range from room temperature to 200 °C. The samples were sealed in glass tube which was heated in oil bath. Each thermal cycling time divided into three segments. The ramp-up heating time was 20 min, the holding time at 200 °C was 10 min, and the cooling time was 50 min, without any holding time. The time of thermal cycling was 80 min in total.
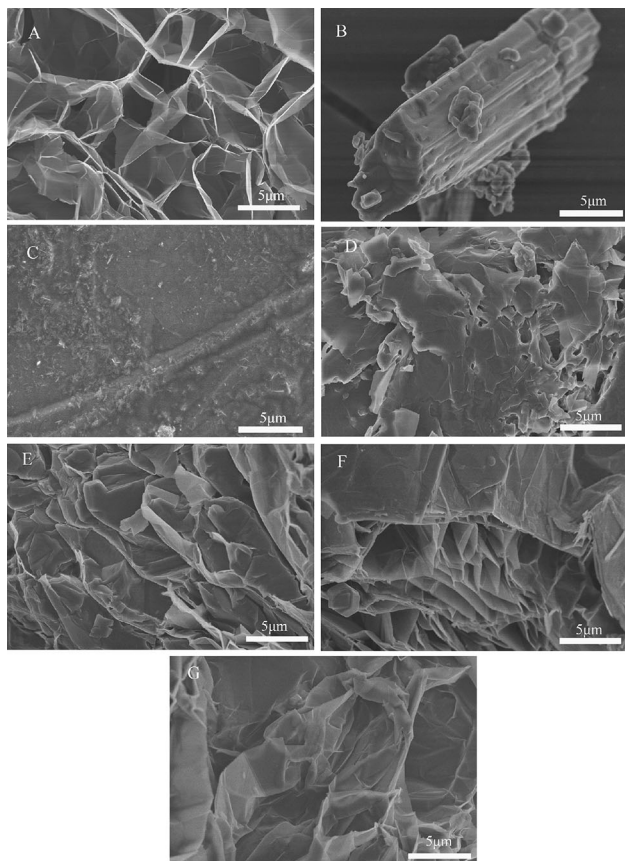
Fig. 1 SEM photographs of the fractured surfaces of **a** pure EG; **b** pure AA; **c** AA-2 mass% EG; **d** AA-4 mass% EG; **e** AA-6 mass% EG; **f** AA-8 mass% EG; **g** AA-10 mass% EG

Fig. 2 XRD spectra of pure AA, EG and its composites

Characterization

The morphologies of composite PCMs were investigated by field emission scanning electron microscopy (FE-SEM, S-4800, Hitachi). Further, the structure and chemical properties of composite PCMs were characterized by X-ray diffraction (XRD, D/MAX-RB, RIGAKU) and Fourier transform infrared spectroscopy (FTIR, Nexus-670, Thermo Nicolet), respectively.

Thermal storage properties of samples including T_m (melting peak temperature), T_f (freezing peak temperature), ΔHm (melting enthalpy) and ΔH_f (freezing enthalpy) were measured by differential scanning calorimeter (DSC, Pyris-1, PE). The calorimeter was calibrated with indium standard before used. The analyses were carried out under a static nitrogen atmosphere and with a heating or cooling rate of 10 °C min^{-1} ranging from 0 to 200 °C. Each sample weighed up to 8 mg and be sealed in a aluminum pan. T_m and T_f of samples were obtained by drawing a line at the point of maximum slope of the leading edge of the DSC curve and extrapolated the base line on the same side of the curve. Furthermore, thermal conductivity of all
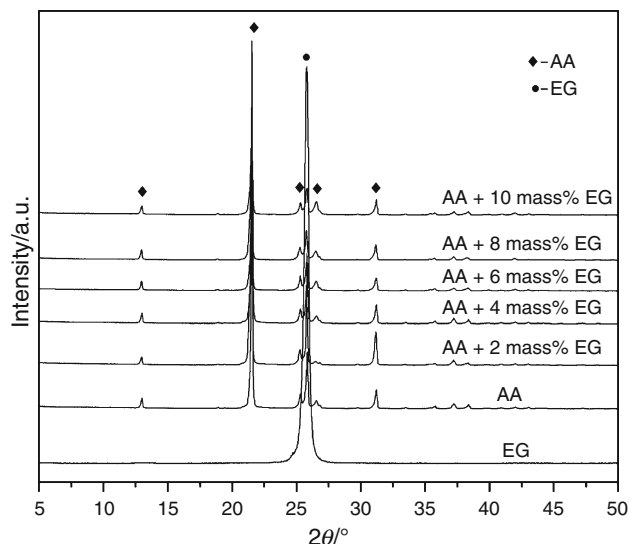
samples was measured by thermal constant measuring instrument (Model 2500S, Sweden) utilizing the transient plane source method.

Results and discussions

Morphology of prepared EG/AA composite PCMs

The morphologies of the fractured surfaces of EG/AA composite PCMs with different EG content are shown in Fig. 1. The pure EG and AA images are shown in Fig. 1a, b, respectively. During the expansion process, EG retains the same structural layer as natural graphite flakes, producing amounts of pores with very large specific surface area. After the EG particles has been striped by ultrasonic irradiation, the lamellar individual EG of about 35 μm of diameter and 80 nm of thickness has been observed. These morphologies were matched with the results in the previous reports [24]. Figure 1c–g presents the morphologies of composite PCMs with various EG contents. It revealed that EG was well dispersed inside the AA matrix, especially the content of EG was relatively low (2 mass%). The morphologies indicated that the method was an effective route to disperse AA into EG.

Structure of prepared EG/AA composite PCMs

The structures of EG, AA and the composites were investigated by XRD, and the results are presented in Fig. 2. It showed the sharp peaks of AA and EG/AA composites appeared at 12.9°, 21.4°, 25.2°, 26.7° and 31.2°, and the results indicated that the structure of AA was
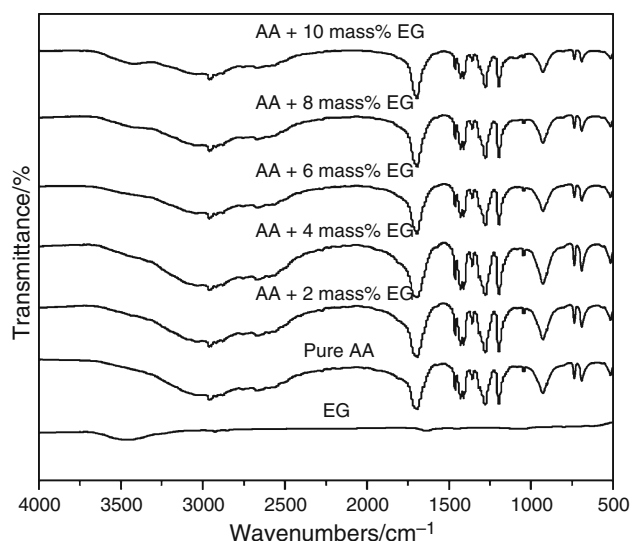
Fig. 3 FTIR spectra of pure EG, AA and composites

Table 2 FTIR spectrum for composite PCMs

Characteristic vibration	Characteristic peaks/cm^{-1}
EG	
C–O stretching	1115 (1098)
C=O stretching	1636 (1633)
C–N stretching	2926, 2843 (2924, 2850)
O–H stretching	3464 (3458)
AA	
Interim –CH$_2$– group	842 (902)
O–H stretching	928 (927)
C–O stretching	1062 (1194)
C=O stretching	1694 (1693)
–CH$_2$– stretching	2887 (2879)
O–H stretching	3033 (3026)

The data in brackets are the corresponding peaks in the pure components

well preserved during the fabrication process. In the EG/AA composites, the sharp peak at 26.4° indicated that the structure of EG was also well preserved during the fabrication process. Moreover, no other impurity peaks were detected from XRD. It can be confirmed that EG and AA preserved their respective structural integrity during the fabrication process, exhibiting well compatibility with each other. The EG and AA were just physically combined with each other in fabrication process.

Figure 3 shows the FTIR spectra of pure AA, EG and the composites. The detailed spectra of compositions are given in Table 2. There were three oxygen-containing groups presented on the spectrum of pure EG at wave numbers of 1098, 1633 and 3458 cm^{-1}, corresponding to

C–O, C=O and O–H stretching vibration, respectively. The result verified the statement reported in the literature that acid intercalation could result in the oxidization of carbon bonds in the surface of graphite. And the presence of the oxygen-containing groups were supposed to be beneficial to the interaction between AA and EG. Comparing the spectra of pure AA, EG and the composites, the spectrum of the composites was mainly organized by all the peaks of its individual component. For instance, the peaks at 1062 and 1115 cm^{-1} present C–O stretching vibration in AA and EG spectra, respectively. It could also be clearly seen in the spectrum of EG/AA composites. The peak at around 3418–3458 cm^{-1} in the spectra of pure EG was O–H stretching peak. In the composites, the spectrum of composites formed an overlapping O–H stretching peaks. In addition, the peak position of the composite PCMs slightly deviated from the original position in their pure spectra. For instance, the carbonyl peaks (C=O) at 1633 and 1638 cm^{-1} in pure EG and AA had been shifted to 1642 cm^{-1} in the composite PCMs. These changes might be caused by the interactions between O–H group in EG and the carbonyl group in EG and AA, which may due to the forming of intermolecular hydrogen bonds. Compared with the spectra of pure AA and EG, the spectrum of EG/AA composites has no obvious new functional groups, which indicated that there is no chemical reaction occurred among the composite PCMs during the fabrication process.

Thermal conductivity of prepared AA and EG/AA composite PCMs

Thermal conductivity of EG/AA composite PCMs with different mass fractions of EG were measured at room temperature. Six specimens of each composite were investigated, and the measurement was repeated to guarantee the accuracy and repeatability. The thermal conductivity results of pure AA and the EG/AA composite PCMs are shown in Fig. 4. It can be seen that the thermal conductivity of the composite PCMs increases greatly with the EG mass fraction. Compared with pure AA (0.45 W m^{-1} K^{-1}), thermal conductivities of the composite PCMs with mass fraction of 2, 4, 6, 8 and 10 mass% EG increased 44.4, 208.9, 224.4, 564.4 and 866.7%, respectively. When the mass fraction of EG was up to 10 mass%, the thermal conductivity of the composite PCMs reached up to 4.35 W m^{-1} K^{-1}, more than 8 times of pure AA. The improvement of thermal conductivity was attributed to the formation of thermal conductive networks in the composites. As can be seen from Fig. 1, amounts of particles gradually connected with each other to form the three-dimensional thermal conductive network which was more dense when the mass fraction of EG increased. The results were consistent with our previous work [25, 26].
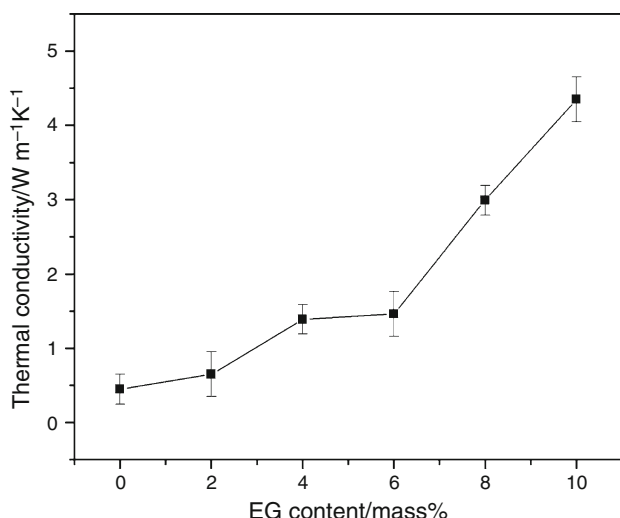
Fig. 4 Experimental thermal conductivity of AA and AA/EG composite PCMs

Fig. 6 Thermal cycles curves of pure AA

The results also showed that the thermal conductivity of AA could be achieved higher when more than 10 mass% of EG was contained. However, this mass fraction is adequate to obtain AA composite PCMs. Once the EG over 10 mass%, the latent heat capacity of the composites will be decreased due to the mass fraction of AA (below 90 mass%). Meanwhile, the EG could not adsorb the AA absolutely. Therefore, the content of EG in the composites was limited in 10 mass%. The high thermal conductivity of EG/AA composite PCMs (about eight times of that of pure AA) makes it much more attractive than pure AA for its passive latent heat thermal energy storage (LHTES) applications.

In order to investigate the heat transfer enhancement effect of EG on composite PCMs, the storage and release experiments were carried out. Figure 5 shows the heat
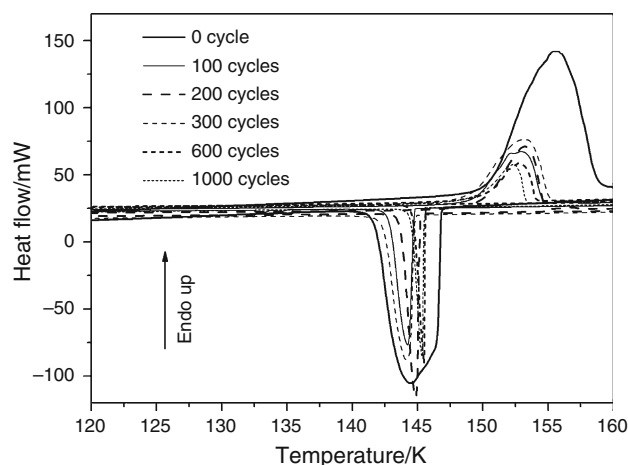
storage and release curves of pure AA and AA/8 mass% EG composites. Compared with the pure AA, the heat storage and release time of AA/8 mass% EG composites decreased to 160 and 200%, respectively. The decrease in the heat storage and release time implies that the EG additive be able to effectively enhance the heat transfer property of the AA.

Thermal properties of AA PCMs

It is known that thermal properties of PCMs such as the melting peak temperature (T_m), freezing peak temperature (T_f), melting enthalpy (ΔH_m) and freezing enthalpy (ΔH_f) were the most important parameters for latent heat thermal energy storage system [27, 28]. The T_m, T_f, ΔH_m and ΔH_f of prepared AA were measured between 0 and 1000 thermal cycles (0th, 100th, 200th, 300th, 600th and 1000th), and DSC curves are shown in Fig. 6. The corresponding
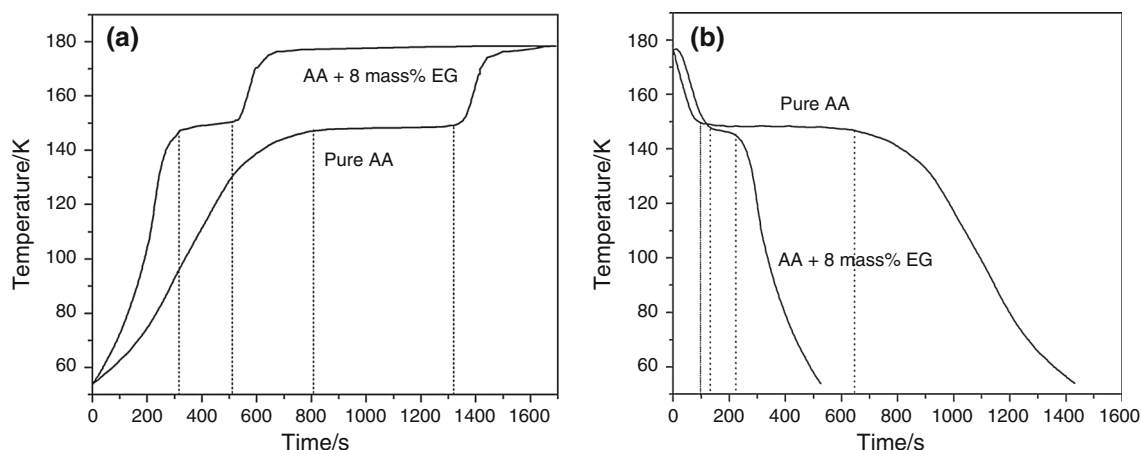

Fig. 5 Heat storage and release curves of AA/8 mass% EG **a** heat storage and **b** heat release

Table 3 Melting peak temperature (T_m), freezing peak temperature (T_f), melting enthalpy (ΔHm) and freezing enthalpy (ΔH_f) of pure AA before and after repeated thermal cycling

S. no	No. of cycles	Melting		Solidification	
		Onset temperature T_m/°C	Latent heat ΔH_m/J g^{-1}	Onset temperature T_f/°C	Latent heat ΔH_f/ J g^{-1}
1	0	150.5	262.6	146.9	255.6
2	100	149.6	237.2	144.7	242.6
3	200	149.9	234.1	145.2	239.3
4	300	149.1	232.1	144.8	233.9
5	600	150.5	224.3	145.6	230.4
6	1000	149.6	220.2	145.5	220.5

thermal characteristics are summarized in Table 3. The values at the 0th cycle were taken as the reference value. Compared with the 0th cycle results of AA, Table 3 shows that the variations of ΔHm were 9.7, 10.9, 11.6, 14.6 and 16.1% after 100th, 200th, 300th, 600th and 1000th cycle, respectively. The values of ΔHm declined with the increasing number of the thermal cycles. As can be seen from Table 3, the T_m and T_f of the pure AA after 1000th thermal cycle were measured as 149.6 and 145.5 °C, changing 1.4 and 2.0 °C, respectively. The ΔH_m and ΔH_f were 220.2 and 220.5 J g^{-1}, changing 16.1 and 13.7%, respectively. Even though, the values were still much higher than other PCM materials. It is revealed that the AA has good stability in thermal properties after 1000 cycles, which makes it as a good candidate in latent heat storage system.

Conclusions

The AA and AA/EG composites were prepared and fabricated in the paper. The AA was used as the PCM material, and EG as the supporting material. Compared with the thermal conductivity of AA (0.45 W m^{-1} K^{-1}), thermal conductivities of the composite PCMs with various mass fraction of 2, 4, 6, 8 and 10% EG increased 44.4, 208.9, 224.4, 564.4 and 866.7%, respectively. The solidification temperature and latent heat of AA were 146.9 °C and of 255.6 J g^{-1}, respectively. Meanwhile, the melting temperature was 150.5 °C, and the latent heat was 262.6 J g^{-1}. After 1000 thermal cycles, the melting and freezing temperature of pure AA were 149.6 and 145.5 °C, respectively. The melting and freezing latent heat were 220.2 and 220.5 J g^{-1}, changing 16.1 and 13.7%, respectively. All the results indicated that the composites have a good thermal stability and can be applied in thermal energy storage system.

References

1. Zalba B, Marin JM, Cabeza LF, Mehling H. Review on thermal energy storage with phase change: materials, heat transfer analysis and applications. Appl Therm Eng. 2003;23(3):251–83.
2. Hadiya JP, Ajit Kumar NS. Experimental thermal behavior response of paraffin wax as storage unit. J Therm Anal Calorim. 2016;124:1511–8.
3. Yu HT, Gao JM, Chen Y, Zhao Y. Preparation and properties of stearic acid/expanded graphite composite phase change material for low-temperature solar thermal application. J Therm Anal Calorim. 2016;124:87–92.
4. Nihal S, Emel O. Organic phase change materials and their textile applications: an overview. Thermochim Acta. 2012;540(20):7–60.
5. Ahmet S, Hayati S, Adem O. Thermal properties and thermal reliability of eutectic mixtures of some fatty acids as latent heat storage materials. Energy Convers Manag. 2004;45:365–76.
6. Ahmet AA, Hasancan O. High-chain fatty acid esters of myristyl alcohol with even carbon number: novel organic phase change materials for thermal energy storage-1. Sol Energy Mater Sol Cells. 2011;95:2752–62.
7. Louis D, Catherine AW, Dominic G, Mary AW. Dodecanoic acid as a promising phase-change material for thermal energy storage. Appl Therm Eng. 2013;53:37–41.
8. Eman-Bellah SM, Ghazy MRA. Thermal conductivity enhancement in a latent heat storage system. Sol Energy. 2007;81:839–45.
9. Xia L, Zhang P. Thermal property measurement and heat transfer analysis of acetamide and acetamide/expanded graphite composite phase change material for solar heat storage. Sol Energy Mater Sol Cells. 2011;95:2246–54.
10. Xiao X, Zhang P, Li M. Preparation and thermal characterization of paraffin/metal foam composite phase change material. Appl Energy. 2013;112:1357–66.
11. Karaipekli A, Sari A, Kaygusuz K. Thermal conductivity improvement of stearic acid using expanded graphite and carbon fiber for energy storage applications. Renew Energy. 2007;32:2201–10.
12. Cai YB, Zong X, Zhang JJ, Du JM, Dong ZD, Wei QF, et al. The improvement of thermal stability and conductivity via incorporation of carbon nanofibers into electrospun ultrafine composite fibers of lauric acid/polyamide phase change materials for thermal energy storage. Green Energy. 2014;11:861–75.
13. Wang J, Xie HQ, Xin Z. Thermal properties of heat storage composites containing multiwalled carbon nanotubes. Appl Phys. 2008;104:113537.1–5.
14. Sharma RKP, Tyagi GVV. Long-term thermal and chemical reliability study of different organic phase change materials for thermal energy storage applications. J Therm Anal Calorim. 2016;124:1357–66.
15. Wang N, Zhang XR, Zhu DS, Gao JW. The investigation of thermal conductivity and energy storage properties of graphite/paraffin composites. J Therm Anal Calorim. 2012;107:949–54.
16. Zhang N, Yuan YP, Wang X, Cao XL, Yang XJ, Hu SC. Preparation and characterization of lauric-myristic-palmitic acid ternary eutectic mixtures/expanded graphite composite phase change material for thermal energy storage. Chem Eng J. 2013;231:214–9.

17. Sari A, Karaipekli A. Preparation, thermal properties and thermal reliability of palmitic acid/expanded graphite composite as form-stable PCM for thermal energy storage. Sol Energy Mater Sol Cells. 2009;93:571–6.

18. Ke HZ, Pang Z, Peng B, Wang J, Cai YB, Huang FL, Wei QT. Thermal energy storage and retrieval properties of form-stable phase change nanofibrous mats based on ternary fatty acid eutectics/polyacrylonitrile composite by magnetron sputtering of silver. J Therm Anal Calorim. 2016;123:1293–307.

19. Fang GY, Li H, Chen Z, et al. Preparation and characterization of stearic acid/expanded graphite composites as thermal energy storage materials. Energy. 2010;35:4622–6.

20. Weiping T, Fei J, Hua Z. Production consumption and development of adipic acid at home and abroad. Chem Intermed. 2005;3:1–4.

21. Zhu J, Qian Y, Zhou W, et al. Adipic acid-silica composite phase change materials for thermal energy storage: preparation and characterization. Energy Storage Sci Technol. 2014;2:123–7.

22. Seki Y, İnce Şeyma, Ezan MA, et al. Graphite nanoplates loading into eutectic mixture of Adipic acid and Sebacic acid as phase change material. Sol Energy Mater Sol Cells. 2015;140:457–63.

23. Liu S, Ma G, Xie S, et al. Diverting the phase transition behavior of adipic acid via mesoporous silica confinement. RSC Adv. 2016;6:111787–96.

24. Guohua C, Wengui W, Dajun W, Cuiling W, Jinrong L, Pingping W, et al. Preparation and characterization of graphite nanosheets from ultrasonic powdering technique. Carbon. 2004;42:753–9.

25. Zhang L, Jiaoqun Z, Weibing Z, Jun W, Yan W. Thermal and electrical conductivity enhancement of graphite nanoplatelets on form-stable polyethylene glycol/polymethyl methacrylate composite phase change materials. Energy. 2012;39:294–302.

26. Lei Z, Jiaoqun Z, Weibing Z, Jun W, Yan W. Characterization of polymethyl methacrylate/polyethylene glycol/aluminum nitride composite as form-stable phase change material prepared by in situ polymerization method. Thermochim Acta. 2011;524:129–35.

27. El-Sebaii AA, Al-Amir S, Al-Marzouki FM, Faidah AS, Al-Ghamdi AA, Al-Henit S. Fast thermal cycling of acetanilide and magnesium chloride hexahydrate for indoor solar cooking. Energy Convers Manag. 2009;50:3104–11.

28. Sari A, Karaipekli A. Fatty acid esters-based composite phase change material for thermal energy storage in buildings. Appl Therm Eng. 2012;37:208–16.